

Emerging Role of Oxidative Stress on EGFR and OGG1-BER Cross-Regulation: Implications in Thyroid Physiopathology

Carmelo Moscatello¹, Maria Carmela Di Marcantonio¹, Luca Savino¹, Emira D'Amico¹, Giordano Spacco¹, Raffella Muraro¹, Gabriella Mincione¹, Roberto Cotellese^{1,2}, Gitana Maria Aceto¹.

¹ Department of Medical, Oral and Biotechnological Sciences, University "G. d'Annunzio" Chieti-Pescara, Via dei Vestini 31, 66100 Chieti, Italy; moscatellocarmelo@gmail.com (C.M.); dimarcantonio@unich.it (M.C.D.M.); luca.sav@hotmail.it (L.S.); emira.damico@unich.it (E.D.A.); giordano.spacco@studenti.unich.it (G.S.); raffaella.muraro@unich.it (R.M.); gabriella.mincione@unich.it (G.M.); roberto.cotellese@unich.it (R.C.); gitana.aceto@unich.it (G.M.A.).

²Villa Serena Foundation for Research, Città Sant'Angelo (Pescara), Italy.

Corresponding author: Gitana Maria Aceto, M.Sc. PhD., Aggregate Professor of General Pathology at the Department of Medical, Oral and Biotechnological Sciences, Gabriele d'Annunzio University of Chieti and Pescara, Via dei Vestini 31, 66100 Chieti, Italy, phone: +39 0871 3554115; gitana.aceto@unich.it

Abstract

Thyroid diseases have a complex and multifactorial aetiology. Despite the numerous studies on the signals referable to the malignant transition, still remain elusive the molecular mechanisms concerning the role of oxidative stress. Based on its strong oxidative power, H₂O₂ could be responsible for the high level of oxidative DNA damage observed in cancerous thyroid tissue and hyper-activation of mitogen-activated protein kinase (MAPK), and PI3K/Akt, that mediate ErbB signaling. Increased levels of 8-oxoG DNA adducts have been detected in the early stages of thyroid cancer. These DNA lesions are efficiently recognized and removed by the base excision repair (BER) pathway initiated by 8-oxoG glycosylase1 (OGG1). This study investigated the relationship between the EGFR and OGG1-BER

pathways and their mutual regulation following oxidative stress stimulus by H₂O₂ in human thyrocytes. We clarified the modulation of ErbB receptors and their downstream pathways (PI3K / Akt and MAPK / ERK) under oxidative stress (from H₂O₂) at the level of gene and protein expression, according to the mechanism defined in a non-pathological cell system, Nthy-ori 3-1. Later, on the basis of the obtained results of gene expression cluster analysis in normal cells, we assessed the dysregulation of the relationships in a model of papillary thyroid cancer with RET/TPC rearrangement (TPC-1). Our observations demonstrated that a H₂O₂ stress may induce a physiological cross-regulation between ErbB and OGG1-BER pathways in normal thyroid cells (while this is dysregulated in the TPC-1 cells). Gene expression data also delineated that *MUTYH* gene could play a physiological role in cross-talk between ErbB and BER pathways and this function is instead lost in cancer cells. Overall our data about OGG1 protein expression suggest that the alternative splicing mechanisms may lead to different protein isoforms, physiologically regulated in response to ErbB modulation, and that these could be dysregulated in the progression of thyroid malignancies with RET/TPC rearrangement.

Short title: ERBB receptors and OGG1-BER crosstalk in thyroid physiopathology

Key words: Oxidative Stress, ERBBs, OGG1, Base Excision Repair, crosstalk, Thyroid

Introduction

Over the last 30 years the incidence rate of thyroid cancer has steadily increased by 2.4 times [1,2] and Papillary Thyroid Carcinoma (PTC) represent the most common histological type with a frequency around 80% of cases [1]. Carcinogenesis and tumor progression in the thyroid gland are a phenotypic expression of a complex molecular interaction based on the connection between gene

predisposition, environmental factors and lifestyle, the effects of which affect the metabolism of the thyroid hormone and DNA oxidative damage [3,4]. Oxidative damage has been suggested to promote tumor initiation and progression by increasing mutation rates and activating oncogenic pathways. The most studied source of oxidative stress is attributable to the reactive oxygen species (ROS) formation, including superoxide anions and Hydrogen Peroxide H_2O_2 [5]. In normal thyroid, H_2O_2 , as stable "diffusible" non-radical oxidant, is produced and consumed in large quantities, because it is required for hormone biosynthesis catalyzed by thyroid peroxidase (TPO) [6,7,8]. On the other hand, based on its strong oxidative power, H_2O_2 , could be responsible for the high level of oxidative DNA damage observed in cancerous thyroid tissue and hyper-activation of signaling pathways [9,10]. In fact, H_2O_2 emerged as major redox metabolite operative in redox sensing, signaling and redox regulation [11]. Intracellular H_2O_2 in cancer cells can regulate EGFR and mitogen-activated protein kinase (MAPK) signaling that contribute to redox-sensitive protein-mediated cancer progression such as EGFR so as promoting cell proliferation [12]. Indeed, because of their detection in thyroid adenomas and in the early stages of cell transformation, it is believed that both oxidative stress and DNA damage are events that precede neoplasia in thyroid cells. Oxidative DNA lesions have also been detected in advanced stages of thyroid cancer, which suggests their contribution in promoting progression to later stages of tumorigenesis [4]. Moreover, high levels of ROS have been reported in thyroid cancer samples along with a decrease in antioxidant enzymes [13] and it has also been proposed that a similar circumstance, present in chronic thyroiditis, could contribute to the development of papillary thyroid carcinoma (PTC) [14]. Of the various types of oxidative DNA damage, 8-oxo-7,8-dihydroguanine (8-oxoG) has been reported as the most abundant, though, it appears to have mild cytotoxicity, its incorporation into DNA may be mutagenic since causes a high transversion mutation rate [15,16,17]. Increased levels of the 8-oxoG DNA adducts have been detected in early stages of thyroid cancer, this may contribute to mutagenesis resulting in increased cell proliferation and survival [18]. The 8-oxoG DNA lesion is recognized and efficiently removed by 8-oxoG glycosylase1 (OGG1)-initiated base excision repair (BER) pathway (OGG1-BER)

[18,19,20]. Along this pathway, the bi-functional glycosylase OGG1 play a pivotal role, together with its partner MUTYH, in the correction of DNA errors, due to the guanines oxidative damage. Therefore, a correct function of OGG1-BER can be considered a protective factor with respect to the triggering of carcinogenic pathways [18,19]. The involvement of EGFR signaling in thyroid carcinogenesis has been documented for a long time [21,22] and a link between DNA repair mechanisms and Epidermal Growth Factor Receptor (EGFR) signaling has been reported in many human tumor cells [23,24,25]; however, their cross-regulation is poorly understood in thyroid tissue pathophysiology. Altered homeostasis in H₂O₂ physiology in thyroid carcinoma cells has been the subject of many studies but, despite of this, the influence in the growth advantage signaling in normal thyrocytes remains controversial, although it has been shown that H₂O₂ is able to cause RET/PTC1 rearrangement which are frequently found in radiation-induced PTCs [26].

All these observations prompted us to investigate the existence of a cross regulation between the molecular pathways connected to the EGFR and BER in thyrocytes. This allowed us to clarify how the modulation of the ErbB receptors and their downstream pathways (PI3K / Akt and MAPK / ERK) under oxidative stress (from H₂O₂) be able to influence gene expression and molecular relationships between the components of the BER signal and the EGF pathway, according to a mechanism defined in a non-pathological cell system. Later, on the basis of the results of gene expression cluster analysis in normal cells, we assessed the dysregulation of the relationships in human model of differentiated thyroid cancer (TPC-1 cell). In order to evaluate how some molecules of EGF-BER cross-talk could be a characteristic of the initial stages involved in the transformation of the thyroid cells towards a papillary lineage.

Materials and Methods

We used two human cell models, Nthy-ori 3-1 as normal thyrocytes and TPC-1 as thyroid papillary cancer cells [27].

Cell Culture and Treatments

Human thyroid follicular epithelial Nthy-ori 3-1 cells, obtained from European Collection of Authenticated Cell Cultures (ECACC 90011609) (Public Health England, Porton Down, Salisbury, UK) (Sigma Aldrich, St. Louis, MO, USA) were cultured at 37°C in RPMI 1640 medium containing 10% Fetal Bovine Serum (FBS), 100U/ml penicillin/streptomycin and 2mM L-glutamine. Human thyroid cancer cell lines, TPC-1 (harboring RET-PTC rearrangement, BRAF WT/WT), characterized according to Schweppe et al., and kindly provided by A. Coppa (Department of Experimental Medicine, Sapienza University of Rome, Rome), were maintained in a 5% CO₂ culture humidified atmosphere, at 37°C in Dulbecco's Modified Eagle Medium (DMEM) supplemented with 10% FBS [28]. For the experiments, cells were grown approximately to 75% confluence, and then the medium was replaced with serum-free medium (medium with 0.2% FBS) overnight in order to reduce basal cellular activity [29]. Then the cells were treated at different times and concentration, with H₂O₂ (Sigma-Aldrich, Milan, Italy) as oxidizing agent alone or combined with 50ng/ml EGF (human recombinant, Sigma Aldrich) or MAPK and AKT inhibitors (PD98059 and LY294002 respectively). For the inhibitors, the cells were pretreated with PD98059 (PD) at 50µM and LY294002 (LY) at 25µM (Cell Signaling Technology, Beverly, MA, USA) for 1 hour.

Cell Viability Assay

To assess the H₂O₂ effects on cell proliferation, cell viability and cytotoxicity, Nthy-ori 3-1 and TPC-1 cells were cultured in 96-well plate (1.0x10⁴ cells/well) and then exposed to H₂O₂ increasing concentration (from 50µM to 10mM) at different times (3, 6 and 24 hours). This was followed by incubation with 10µl/well of 2-[2-methoxy-4-nitrophenyl]-3-[4-nitrophenyl]-5-[2,4-disulphophenyl]-2H-tetrazolium, monosodium salt (MTS) assay (Promega, Madison WI, USA) at 37°C for 1 hour. Cell viability was evaluated at 490nm using the GloMax-Multi Detection System (Promega).

Real-Time Quantitative PCR Analysis (qRT-PCR)

Total RNA was isolated from Nthy-ori 3-1 and TPC-1 cells treated with 10 mM H₂O₂ and LY, PD and EGF alone and combined as specified in “Cell Culture and treatments”, using TriFast (EUROGOLD EuroClone) according to the manufacturer’s instructions. The synthesis of complementary DNA (cDNA) was performed as previously described [30]. The mRNA levels were evaluated by SYBR Green quantitative real-time PCR (qRT-PCR) analysis using StepOne™ 2.0 (Applied Biosystems, Thermo Fisher Scientific, Waltham, MA, USA). Data were analyzed using the comparative Ct method and were graphically indicated as $2^{-\Delta\Delta C_t} + SD$. In accordance with the method, the mRNA amounts of the target genes were normalized by the ratio on the median value of the endogenous housekeeping gene (*GUSB*) obtained in each treated cells vs untreated (quiescent) cells. Targets and reference genes were amplified in triplicate in a volume of 10µl containing 1µl template cDNA, 0.2µl of primers mixture and 5µl of GoTaq® 2-Step RT-qPCR System (Promega) according to the manufacturer’s instructions. Primers sequences are available in **Table S1**.

The cycling conditions were performed as follows, 10 minutes at 95°C and 40 cycles of 15 seconds at 95°C followed by 1 minute at 60°C and final elongation of 15 seconds at 95°C.

Gene dosage assay of *OGGI* and *MUTYH*

Two different genomic target sequences were selected for *OGGI* (GeneID: 4968; Gene Bank accession number: NM_016821) and *MUTYH* (GeneID: 4595; Gene Bank accession number: NM_12222.1). Genomic DNA was extracted as previously described [30] and gene dosage was performed by SYBR Green qRT-PCR. The samples were amplified in triplicate in three independent experiments. Data were analyzed using $2^{-\Delta\Delta C_t} + SD$. In accordance with the qRT-PCR method, previously described, the gDNA amounts of the target genes were normalized by the ratio on median value of the *B-Actin* as genomic reference from TPC-1 vs Nthy-ori 3-1. Primers sequences are listed in **Table S1**.

Western Blotting

Total proteins were isolated from Nthy-ori 3-1 and TPC-1 cells treated with 10 mM H₂O₂ and LY, PD and EGF as specified in “Cell Culture and treatments” and were extracted using lysis buffer [2mM

Na₃VO₄, 4mM sodium pyrophosphate, 10mM sodium fluoride, 50mM HEPES pH 7.9, 100 mM NaCl, 10mM EDTA, 1% Triton X-100, 2µg/ml leupeptin, 2µg/ml aprotinin, 1mM PMSF]. Protein concentrations were determined using the BCA protein assay (Thermo Fisher Scientific). An equal amount of total proteins was separated on 4-20% SDS-PAGE pre-cast gel electrophoresis (Bio-Rad Laboratories, Hercules, CA, USA) and transferred onto PVDF membranes (GE Healthcare, Chicago, IL, USA). Then, after blocking, the membranes were incubated with primary antibody overnight at 4°C. The following primary antibodies were used: phospho-p44/42 MAPK, phospho-AKT, phospho-EGFR (Tyr1068), PARP-1 (Cell Signaling Technology); EGFR (Santa Cruz Biotechnology, Santa Cruz, CA, USA); ErbB2 (Dako, Santa Clara, CA, USA); OGG1 (Novus Biologicals, Littleton, CO, USA); β-actin (Sigma-Aldrich, St. Louis, MI, USA) was used as a protein loading control. Secondary antibodies were HRP-conjugated anti-rabbit or anti-mouse (Bethyl Laboratories, Montgomery, TX, USA). The immune complexes were visualized using the ECL Western blot detection system (EuroClone). Protein amounts were quantified by the Image Lab™ Software Version 5.0 (Bio-Rad Laboratories)

Statistical Analysis and Tools.

All measurements were made after three independent experiments, and for each data is shown a representative value of all experiments plus standard deviation. The results were subjected to t-test or one-way analysis of variance (ANOVA) as appropriate. All *p* values are two-sided and a *p* value of less than 0.05 was considered significant. All analyses were performed using SPSS software. The program Multiexperiment viewer v4.9.0 (MeV4.9.0) [31] was employed to elucidate molecular relationship among genes expression detected in the normal Nthy-ori 3-1 cells in response to the treatments.

Results

Cell line viability after Hydrogen Peroxide (H₂O₂) treatment

After hydrogen peroxide (H₂O₂) treatment we observed a time-independent fast declined in cell viability ($p < 0,001$) in both cell lines. In the normal (Nthy-ori 3-1) cells the viability settled on a constant value (about 50%) for all concentration and times. (**Figure 1A**). Whereas, TPC-1 viability after H₂O₂ treatment attested from 60% to 40% after 3, 6 and 24 hours (**Figure 1B**). Furthermore, H₂O₂ induced the recovery of the TPC-1 cell viability for the three treatment times, unlike normal cells.

Gene expression of BER and EGF signalling in Nthy-ori 3-1

Gene expression modulation of BER and EGF signalling was assayed in human thyroid follicular epithelial Nthy-ori 3-1 cells, at different times, after treatments with H₂O₂ as oxidizing agent, EGF, PD98059 (PD) and LY294002 (LY) alone or combined with H₂O₂. The BER genes: *OGGI*, *MUTYH*, *APE-1/Ref-1* and *PPARg* (**Figure 2 A, B, C, D**), exhibited generally the same trend in the different experimental conditions. These genes showed a significant ($p < 0.05$) time-depend increase, after H₂O₂ treatment, and a significant ($p < 0.05$) decrease when the cells were stimulated by EGF and after inhibition of AKT and MAPK signalling (by LY and PD respectively). Except for *PPARg* gene expression, that unlike the other BER genes, did not changed after inhibition by PD (**Figure 2D**). EGF and H₂O₂ co-treatment increased *OGGI*, *MUTYH* and *PPARg* compared to EGF treatment alone; this was not observed for APE-1 gene expression.

The Nuclear Factor (erythroid-derived 2)-like 2, *NRF2* decreased with EGF, LY and PD (alone and combined with H₂O₂) (**Figure 2E**). The inhibition by PD and PD+H₂O₂ after 30 minutes increased the expression of protective antioxidant gene *HO1*, that conversely was decreased by EGF and LY inhibitor (**Figure 2F**). Stimulation with EGF and H₂O₂, alone or in combination, did not induce any modulation of *EGFR* expression; while LY and PD determined its overexpression and furthermore H₂O₂ strengthened the action of inhibitors (**Figure 2I**). ErbB2 expression did not show any modulation by H₂O₂ alone whereas it resulted inhibited by EGF and LY and increased by EGF and

H₂O₂ co-treatment and MAPK inhibition. (**Figure 2J**). *ErbB3* resulted stimulated by EGF and PD treatments also combined with H₂O₂ (**Figure 2K**). In all conditions *ErbB4* was not detected, except after EGF stimulation (data not shown) (**Figure 2K**). The transcription factor *JUN/AP1* did not show any modulation following H₂O₂, LY and PD treatments, while its expression was increased by EGF (**Figure 2G**). In Nthy-ori3-1 the pro-inflammatory CXC chemokine IL-8 gene (*CXCL8*) was significantly increased in proliferating cells compared to starved cells and in particular after H₂O₂ treatments; whereas its expression was reduced by EGF stimulation and its downstream pathways (AKT and MAPK) inhibition (**Figure 2H**). As expected, the expression of stem cell regulator *ZEB1* increased in proliferating cells, after EGF stimulation and also in oxidative stress conditions. While its expression was decreased by LY and H₂O₂ co-treatment. Thyroid differentiation marker *TPO* showed an opposite trend in gene expression compared to *ZEB1*, except for the treatment with H₂O₂ (**Figure 2N**). The reduction of *TPO* gene expression was detected following the inhibition of the AKT pathway while a contrary effect was obtained after MAPK inhibition (**Figure 2M**).

Gene expression cluster analysis in Nthy-ori 3-1

To elucidate the potential cross-regulation between BER and EGFR pathways, we compared the genes expression levels detected in Nthy-ori 3-1 cells in response to the several treatments employing Multiexperiment viewer v4.0 program (MeV4.0) [31] (**Figure 3**). Under acute oxidative stress conditions (by 10mM H₂O₂ treatment), a close correlation among genes involved in stress response, i.e. *MUTYH*, *HO1* and *OGG1*, was observed. We also highlighted the correlation among *TPO*, IL-8 and *JUN/AP1* transcription factor (**Figure 3A**).

When Nthy-ori 3-1 cell line was stimulated by EGF, a strong relationship among the BER genes, *OGG1* and *APE1/Ref1* (alternatively named *APEX1*, *HAP1*, *APEN*), and antioxidant response gene, *NRF2* and *OH1* was shown; whereas *MUTYH* and *PPARg* showed a correlation with *ErbB2* (**Figure 3B**). The inhibition of AKT pathway by LY, highlighted a lack of BER gene correlation, in addition *APE1/Ref1* was related to *NRF2*, *HO1* IL-8 and also to *ErbB2* (**Figure 3C**). Interestingly, in normal

thyroid cells the inhibition of MAPK (by PD) was the unique experimental condition that showed a correlation among the ErbB receptors (**Figure 3D**).

Gene expression deregulation of BER and EGF signalling in TPC-1 tumor cells

Respect to normal cells (Nthy-ori 3-1), the TPC1 tumor cells showed an overall gene expression deregulation, in response to the treatments (**Figure 4 vs Figure2**). Indeed, an increase in expression after AKT inhibition was observed for *OGGI* and *APE1*, while only *APE1* showed an overexpression after stimulation by EGF (**Figure 4 A, B**). *MUTYH* expression was detected only after 15 minutes H_2O_2 treatment alone and in combination with EGF (data not shown). Following stimulation with H_2O_2 , EGF and PD an increase of *JUN/API* transcription factor expression was observed, while it resulted downregulated after AKT inhibition (**Figure 4C**). An aberrant modulation of the *EGFR*, *ERBB2* and *ERBB3* genes was also observed in TPC-1 cells. In fact, these genes tended to be repressed or poorly expressed (even in proliferating cells) but they resulted stimulated by MAPK inhibition combined with oxidative stress (**Figure 4 D, E, F**). The expression of zinc finger *ZEB1* increased after LY and PD treatments while oxidative stress reduced its expression (**Figure 4 G**). In all experimental conditions, thyroid differentiation marker *TPO* resulted undetected (data not shown).

Gene dosage assay of *OGGI* and *MUTYH* in TPC1cells.

Since TPC-1 cells did not express *MUTYH*, we evaluated the amount of genomic DNA (gDNA) of this gene and its partner *OGGI*. The qPCR data were normalized by the ratio on the value of endogenous *B-Actin* gDNA. The reference amount of the both alleles presence was validated on gDNA from Nthy-ori 3-1 cells; since the normalized values of the controls (cell lines) matched perfectly, we were confident to employ this method to assay the TPC-1 cell line genome. In the TPC-1 cells *OGGI* and *MUTYH* gDNA value did not show reduction (**Figure 5**).

Protein expression of ErbB pathway and *OGG1* in NThy-ori 3-1 and TPC-1 cells

At this point we also assessed, in normal and cancer cells, the response induced by an H_2O_2 stress on ErbB pathways and *OGG1*.

Western blotting analyses showed that the OGG1 protein was expressed in quiescent Nthy-ori 3-1 cells, with two clearly visible bands, at approximately 47 kDa and 22 kDa (**Figure 6C**) [32]. These two OGG1 isoforms were reduced or absent after H₂O₂ treatments alone or combined with AKT and MAPK inhibitors (LY and PD respectively). Instead, the same bands were observed after LY, PD and EGF treatment (**Figure 6A**), while EGF and H₂O₂ co-treatment seemed to induce further OGG1 post-translational modifications, thus allowing the detection of many isoforms (**Figure 6C**).

The 39 kDa band, which should correspond to the nuclear isoform (1a) [32] was always present, whereas the EGF and H₂O₂ co-treatment caused an increase in its expression. The level of PARP-1 protein expression was very mild in quiescent Nthy-ori 3-1 cells and the oxidative stress did not seem to modulate it. On the contrary, the treatments with LY, PD and EGF caused an increase in PARP-1 expression, which then decreased with the addition of H₂O₂. Interestingly, under all the experimental conditions we use, this protein resulted not cleaved, indicating that apoptosis (PARP-1 dependent) has not been activated (**Figure 6C**).

Unlike that was observed in normal Nthy-ori 3-1, in the papillary thyroid carcinoma model (TPC1) H₂O₂ increased OGG1 expression after MAPK and AKT pathways inhibition, the stimulation by EGF did not cause relevant changes respect to untreated quiescent cells (**Figure 6D**). Furthermore, EGF in combination with H₂O₂, in TPC1 seemed to stimulate only the expression of the higher molecular weight OGG1 isoform (**Figure 6D**). The 39kDa nuclear isoform showed a low expression in quiescent TPC1 and after AKT inhibition while increased after MAPK inhibition.

In quiescent tumor cells, PARP 1 was induced by EGF stimulation and inhibition of its downstream pathways (**Figure 6D**).

In Nthy-ori 3-1 cell line, the protein level of EGFR remained unchanged upon all treatments (data not shown), while as expected, its phosphorylation in Tyr1068 was absent in the quiescent untraded cells and appeared after EGF stimulation (**Figure 6A**). The acute stress by H₂O₂ always induced EGFR phosphorylation even after inhibition of the AKT and MAPK. In all experimental conditions, ErbB2 was expressed and slightly reduced following oxidative stress (**Figure 6A**). In quiescent cells, MAPK

phosphorylation was observed, while it was lightly inhibited by treatment with LY alone and with EGF plus H₂O₂. Interestingly, PD and H₂O₂ co-treatment increased MAPK phosphorylation compared to PD alone. In quiescent untreated cells a high level of phospho-AKT was detected and H₂O₂ treatment, after 30', inhibited it so as to be undetected. PD treatment led a decrease of AKT phosphorylation which was more pronounced after co-treatment with H₂O₂.

Papillary thyroid cancer model TPC-1 did not express p-EGFR under any of the tested conditions (data not shown), whereas ErbB2 protein was always expressed and particularly increased after PD and EGF alone treatments (**Figure 6B**). The MAPK were activated in all experimental conditions especially with LY and H₂O₂ co-treatment, contrary to what observed in normal cells. AKT was activated in the presence of H₂O₂ also with PD and EGF alone.

Discussion

Thyroid diseases have a complex and multifactorial etiology [33]. Despite the numerous studies on the signals referable to the malignant transition [3], remain still elusive the molecular mechanisms concerning the role of oxidative stress in diseases and carcinogenesis of thyroid. Indeed, it has long been believed that oxidative stress plays an active role in carcinogenesis [5]. One of the molecules with pro-oxidant characteristics is H₂O₂. Although it is physiologically produced in the thyroid, it is also involved in the adaptation to stress and in chronic inflammatory responses [1,10], but it is also actively produced in the thyroid as necessary for thyroid hormone synthesis. However, there are still many gaps in our knowledge regarding the cellular signaling network attributable to H₂O₂ and to DNA damage in thyroid. Based on its strong oxidative power, H₂O₂ could be responsible for the high level of oxidative DNA damage observed in cancerous thyroid tissue [14] and hyper-activation of some signaling pathways [10] including mitogen-activated protein kinase (MAPK), and PI3K/Akt, that mediate ErbB signaling [12, 34]. In this study we investigated the relationship between the EGFR and BER pathways and its regulation following acute oxidative stress stimulus by H₂O₂. We first assessed the physiological relationships between the two pathways using gene expression on a normal

thyroid cell line (Nthy-ori 3-1), then we verified the dysregulations of these signals in TPC-1 tumor cells. In both thyroid cell models, viability fast declined in a time-independent manner, after H₂O₂ treatment, whereas TPC-1 cells displayed a recovery for short times of treatment (**Figure 1B**) demonstrating the ormetic properties of H₂O₂ [35] in this model of papillary tumor. In thyrocytes the TPO downregulation, reducing its H₂O₂ chemo-protective function, is involved in the evolution of nodularity towards the condition of tumorigenesis [36], in TPC-1 the expression of TPO was not detected. H₂O₂, is a crucial substrate for thyroid peroxidase (TPO), a key enzyme involved in thyroid hormone synthesis [8]. On the plasma membrane of thyrocytes, TPO is associated with oxidoreductase dual oxidase 2 (DUOX2) and this functional interaction is essential for the regulation of the extracellular H₂O₂ level [8].

In this study we highlighted the cross-talk effect between EGFR and OGG1-BER on gene expression modulation, by stimulating thyroid cells with H₂O₂ and EGF, and inhibiting EGFR its downstream ways, AKT and MAPK, using LY and PD (respectively).

Nthy-ori 3-1 cells were treated with H₂O₂, EGF, LY and PD alone and in combination. We observed that expression of genes involved in BER pathway, i.e. *OGG1*, *MUTYH*, *APE-1/Ref1* and *PPARg*, exhibited generally the same trend, resulting upregulated by H₂O₂ and downregulated by LY and PD. The *NRF2* gene expression decreased with EGF, LY and PD (with and without H₂O₂), while in contrast *OGG1* increased. This suggested that in thyroid *OGG1* may be regulated by a NRF2-independent way, in spite of the presence of an ARE (Antioxidant Response Elements) region recognized by NRF2 in *OGG1* promoter [37]. In addition, the expression of the *HO1* gene, which responds both to oxidative stress and to NRF2-mediated gene regulation in different tissues [38], displayed a different behaviour respect to *NRF2*. These data did not completely exclude a role of NRF2 transcription factor in the response to acute oxidative stress in our system, because it is well-known that there are inactive form resides as subcellular compartmentalization pool bounded to Keap1 [39].

When Nthy-ori 3-1 cells were stimulated with EGF and H₂O₂, *OGG1* and *APE1/Ref1* showed a strong correlation with *NRF2* and its downstream *HO1* and *IL8*. Instead, *MUTYH* demonstrated a correlation with *ErbB2* and *PPARg* (**Figure 3B**).

After LY treatment no significant correlation between any of the BER genes was shown. Interestingly, the experimental inhibition of MAPK (with PD) was the unique experimental condition we observed a correlation among ErbB genes that suggest a positive feedback mechanism.

Our results highlighted that the inhibition of ErbB receptors downstream pathways may have a role in dysregulation of the BER genes.

After inhibition of the AKT pathway, a correlation was observed between *OGG1* and *JUN/AP1* while after MAPK inhibition, they correlated with CXC chemokine *IL-8* (also *CXCL8*) and *JUN/AP1* as reported in the literature [40]. Therefore, the JUN/AP1 transcriptional activator could play a pivotal role in the correlation between the ErbB and BER systems (**Figure 3**).

Pro-inflammatory CXC chemokine *IL-8* (*CXCL8*) gene expression was significantly increased in Nthy-ori 3-1 proliferating cells and after H₂O₂ treatments compared to starved cells. On the contrary *IL-8* was reduced after EGF, LY and PD treatments alone and combined with H₂O₂ (**Figure 2H**). Our data confirmed that *IL-8* plays a role in response to oxidative stress that also stimulate its own production [41]. It is interesting to highlight that its synthesis depends, at least in part, by EGFR activation [42]. *IL-8* was the first demonstrated chemokine to be secreted by human normal thyrocytes [43]. Moreover, the secretion of *IL-8* by cancer cells can enhance the proliferation and survival capabilities through an autocrine loop [42]. *MUTYH* gene in Nthy-ori 3-1 cells was clustered with other BER genes under oxidative stress conditions whereas EGF induced a correlation with *PPARg* and *ErbB2* (**Figure 3B**), but this correlation was lost after LY and PD treatment suggesting that *MUTYH* gene expression might be regulated by EGFR pathways. Furthermore, gene expression data underlined a close correlation among *MUTYH*, *HO1* and *OGG1*, following H₂O₂ treatment. In contrast, following EGF treatment, a close correlation among *MUTYH*, *PPARg* and *ErbB2* was shown. These results confirmed the relationship between ErbB2 and PPARg in regulating cell

proliferation and metabolism as already displayed in other tissues [44]. It also highlights a bivalent role for *MUTYH*, under acute oxidative stress condition *MUTYH* showed a correlation with the other BER genes, probably because the primary necessity of cells is to defend itself from the high level of oxidative stress. Whereas, after EGF growth stimulus *MUTYH* showed a correlation with ErbB2 and PPAR γ likely due to an increase in the metabolism rather than DNA repair, which becomes a secondary mechanism.

In Nthy-ori 3-1 cells, EGF treatment increased *ErbB2* gene expression only in combination with H₂O₂. The same effect was observed by blocking MAPK pathway by PD (**Figure 2J**). Under the effect of LY and PD cotreated with H₂O₂ EGFR expression increased significantly (**Figure 2I**). These data were confirmed by protein analysis showing changes in EGFR receptor activation after H₂O₂ treatment without altering its expression (**Figure 6A**). These results led us to suggest the presence of fine-tuned mechanisms that regulate signals downstream of EGF and cross-talk with activities controlled by OGG1 protein. The simultaneous presence of a factor that stimulates cellular growth (i.e. EGF) and adaptation to the oxidative stress, H₂O₂-mediated, induced the expression of different isoforms of the OGG1 in these cells. Our results showed that OGG1 protein in normal thyroid cells was expressed in several isoforms depending on the treatments used (**Figure 6C**). These findings could be explained both on the basis of that is currently known about this enzyme; an alternative splicing mechanism that act on the C-terminal region was delineated. As a consequence, all isoforms share the N-terminal region but differ in C-terminal, determining the existence of several isoforms, such as the alternative splicing process of the C-terminal region of OGG1 [32] and on post-translational modifications occurred as a response to the stress [45]. Currently, most of the activities of these isoforms are unknown. The OGG1 N-terminal region could be directly linked by PARP-1 and this interaction is enhanced by oxidative stress [46]. In our system LY, PD and EGF treatment caused an increase in PARP-1 protein expression. It is already known that, both in presence and in absence of damaged DNA, the catalytic activity of PARP-1 is significantly enhanced and maximized

by action of phosphorylated MAPK [47]. This suggest that PARP-1 may interact with AKTsignal as well as MAPK and it could have a role in cross-talk with BER.

In the normal system, OGG1 was shown to be controlled by the AKT pathway as it also decreased in protein level, while stimulation with EGF increased its expression in many of its isoforms (**Figure 6 C**). Our results highlighted that the inhibition of ErbB receptors downstream pathways may have a role in modulation of the OGG1 end BER system. This aspect is very dysregulated in the TPC-1 tumor cell which shows a strong expression of OGG1 despite the inhibition of AKT (**Figure 6 D**). Although OGG1-BER protects the genome integrity by repairing the lesion or eliminating cells with malignant potential and its overexpression improves H₂O₂-induced cell death [20], in the case of TPC-1, the lack of *MUTYH* gene expression could favour the maintenance of tumor phenotype loop [48]. Furthermore, this confirms that OGG1, as a sensor in the BER response, can be controlled both at the gene and protein level by the Pi3K / AKT pathway while this was not detected following stimulation by EGF and H₂O₂, which also repressed the PARP1 expression. Probably in quiescent TPC-1 the presence of the RET/PTC rearrangement keeps the growth pathways independent of EGF stimulation by not expressing pEGFR as it appears to be (albeit slightly) in TPC-1 proliferating cells [49]. Molecular studies have also shown that RET/PTC in human thyrocytes promotes the activation of inflammation-related genes expression and this could contribute to the progression and locoregional metastases, characteristic of the PTC tumors [50]. Stimulation of the OGG1 isoforms could also be caused by this aspect. Indeed, some studies have shown that the 8-oxoguanin glycosylase-1 repair enzyme is also involved in inflammation regulation and diseases [51-54].

TPC-1cells showed a strong deregulation of the BER, OGG1 and *MUTYH*, components (**Figure 4**) with a loss in the gene expression of *MUTYH* and an increased expression of *APE-1 /Ref1*. This result could be due to the presence of the RET/TPC rearrangement in the papillary tumor model, indeed, oncogenic potential of RET/PTC is related to intrinsic tyrosine kinase activity and repression of p53-dependent transactivation [55]. Moreover, some previous studies have shown that the gene expression of *MUTYH* is controlled by TP53 [56] and that TP53 can also modulate the

transcriptional activity of APE-1/Ref1 [57]. At present, these interactions between tyrosine kinase activities and BER signaling modulations have not yet been adequately explored in thyroid carcinogenesis and deserve further studies.

Conclusion

Our observations demonstrated for the first time the evidence that a pronounced stress with H₂O₂ may induce a physiological cross-regulation between ErbB and BER pathways in normal thyroid epithelial cells while this is dysregulated in the TPC-1. Gene expression data also delineated that *MUTYH* gene may play a physiological role in cross-talk between ErbB and BER pathways and that this function is instead lost in cancer cells. Overall data about OGG1 protein led us to suggest that the alternative splicing mechanism that leads to the expression of the several OGG1 protein isoforms could be physiologically regulated in response to different exogenous and/or endogenous signals, but also it could be dysregulated in different way according to the progression of malignancy in thyroid diseases. Finally, this study revealed the need to investigate the still open questions concerning the pathophysiological crosstalk between ErbB and BER pathways to better shed light on the mechanisms underlying the onset and development of thyroid pathologies.

ABBREVIATIONS

AKT (Protein Kinase B)

BER (Base Excision Repair)

DUOX2 (Dual Oxidase 2)

APE1/Ref1 (Apurinic/Apyrimidinic Endodeoxyribonuclease-1;

EGFR (epidermal growth factor receptor);

ErbB2 (Erb-B2 receptor tyrosine kinase 2);

ErbB3 (Erb-B3 receptor tyrosine kinase 3);

ErbB4 (Erb-B4 receptor tyrosine kinase 4);

GUSB (Glucuronidase Beta)

HO1 (Heme Oxygenase 1);

IL8 (CXCL8, Interleukin 8);

Jun/AP1 (Jun proto-oncogene, AP-1 transcription factor subunit)

LY: LY294002;

MAPK (Mitogen-Activated Protein Kinase)

MUTYH (mutY DNA glycosylase);

NRF2 (Nuclear Factor, Erythroid 2 like 2);

OGG1 (8-Oxoguanine Glycosylase-1);

PPAR γ (Peroxisome Proliferator Activated Receptor gamma);

PTC (Papillary Thyroid Carcinoma)

ROS (Reactive Oxygen Species)

TPO (Thyroid Peroxidase);

ZEB-1 (Zinc finger E-box Binding homeobox 1)

PD: PD98059

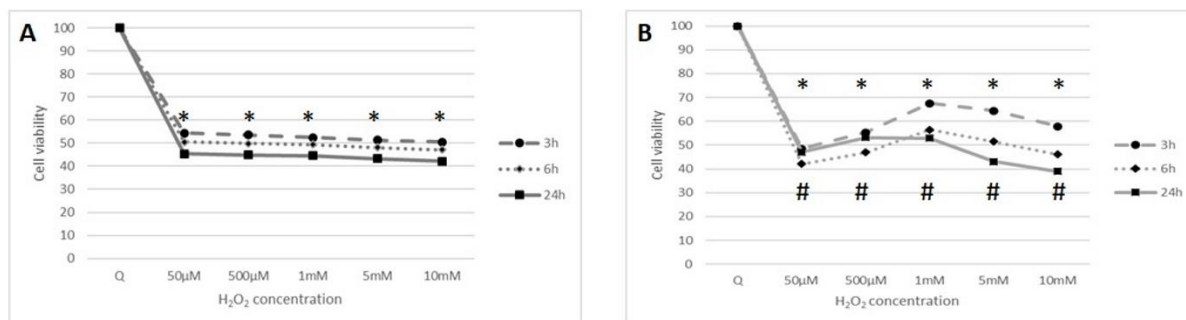


Figure 1. Nthy-ori 3-1 (A) and TPC-1 (B) cell line viability under oxidative stress condition.

Cell viability was assayed using MTS. Cells were exposed to Hydrogen Peroxide (H_2O_2) as oxidizing agent for different time and concentrations (from 50 μM to 10 mM). For each experiment $n=5$ replicates wells were assayed per clone. Cell viability values were calculated as means and compared to untreated quiescent cells (Q). * $p < 0.001$ vs quiescent; # $p < 0.001$ cells with same dosage of H_2O_2 treatment at different time.

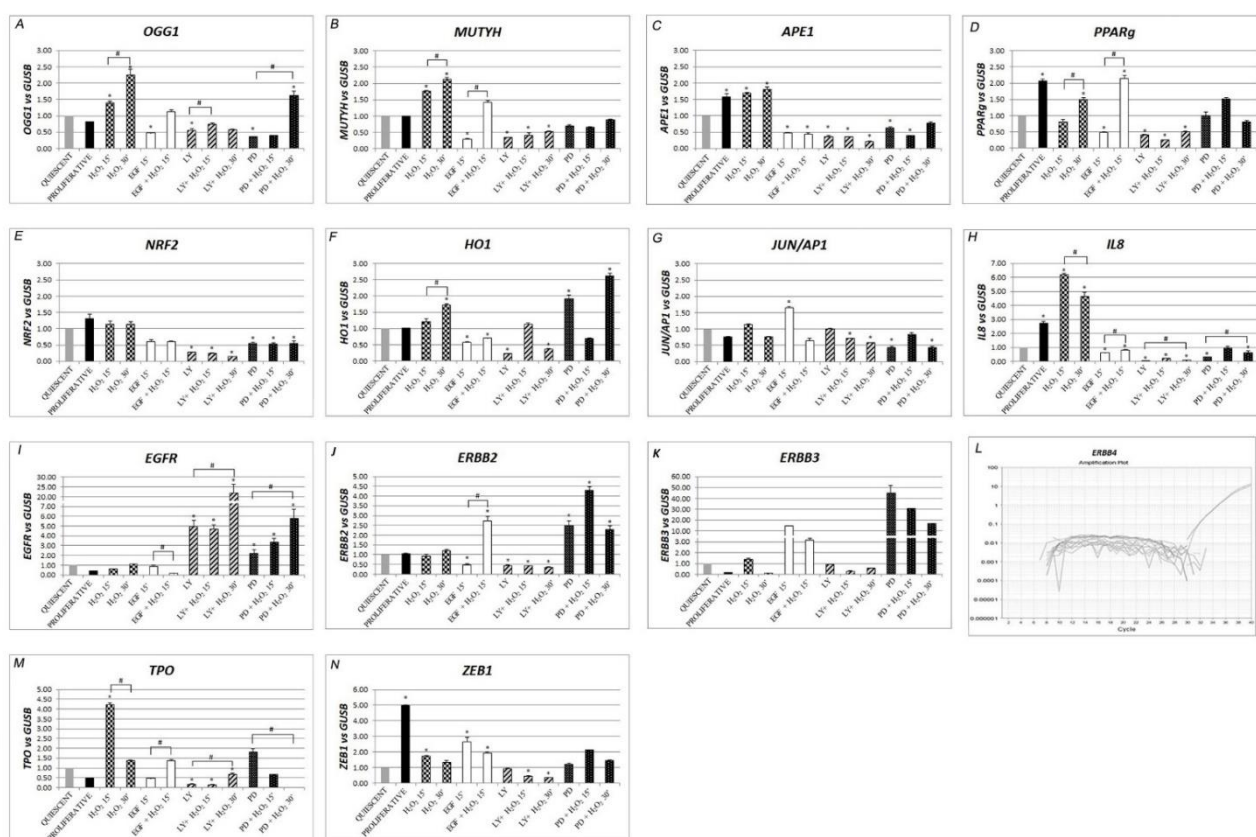


Figure 2. Gene expression modulation under H₂O₂, EGF, LY and PD treatments alone and combined in Nthy-ori 3-1 cells. Gene expression was analysed by Real Time-qPCR. The histogram represented normalized data with GUSB gene, and the results showed the average of three independent experiments. **(A)** *OGG1* (8-Oxoguanine glycosylase); **(B)** *MUTYH* (mutY DNA glycosylase); **(C)** *PPARγ* (peroxisome proliferator activated receptor gamma); **(D)** *APE1* (apurinic/apyrimidinic endodeoxyribonuclease-1); **(E)** *NRF2* (nuclear factor, erythroid 2 like 2); **(F)** *HO1* (heme oxygenase 1); **(G)** *JUN/AP1* (Jun proto-oncogene, AP-1 transcription factor subunit); **(H)** *IL8* (CXCL8, interleukin 8); **(I)** *EGFR* (epidermal growth factor receptor); **(J)** *ERBB2* (Erb-B2 receptor tyrosine kinase 2); **(K)** *ERBB3* (Erb-B3 receptor tyrosine kinase 3); **(L)** *ERBB4* (Erb-B4 receptor tyrosine kinase 4); **(M)** *TPO* (thyroid peroxidase); **(N)** *ZEB-1* (zinc finger E-box binding homeobox 1). LY: LY294002; PD: PD98059

* $p < 0.05$ treated vs quiescent cells; # $p < 0.05$ cells with similar treatment.

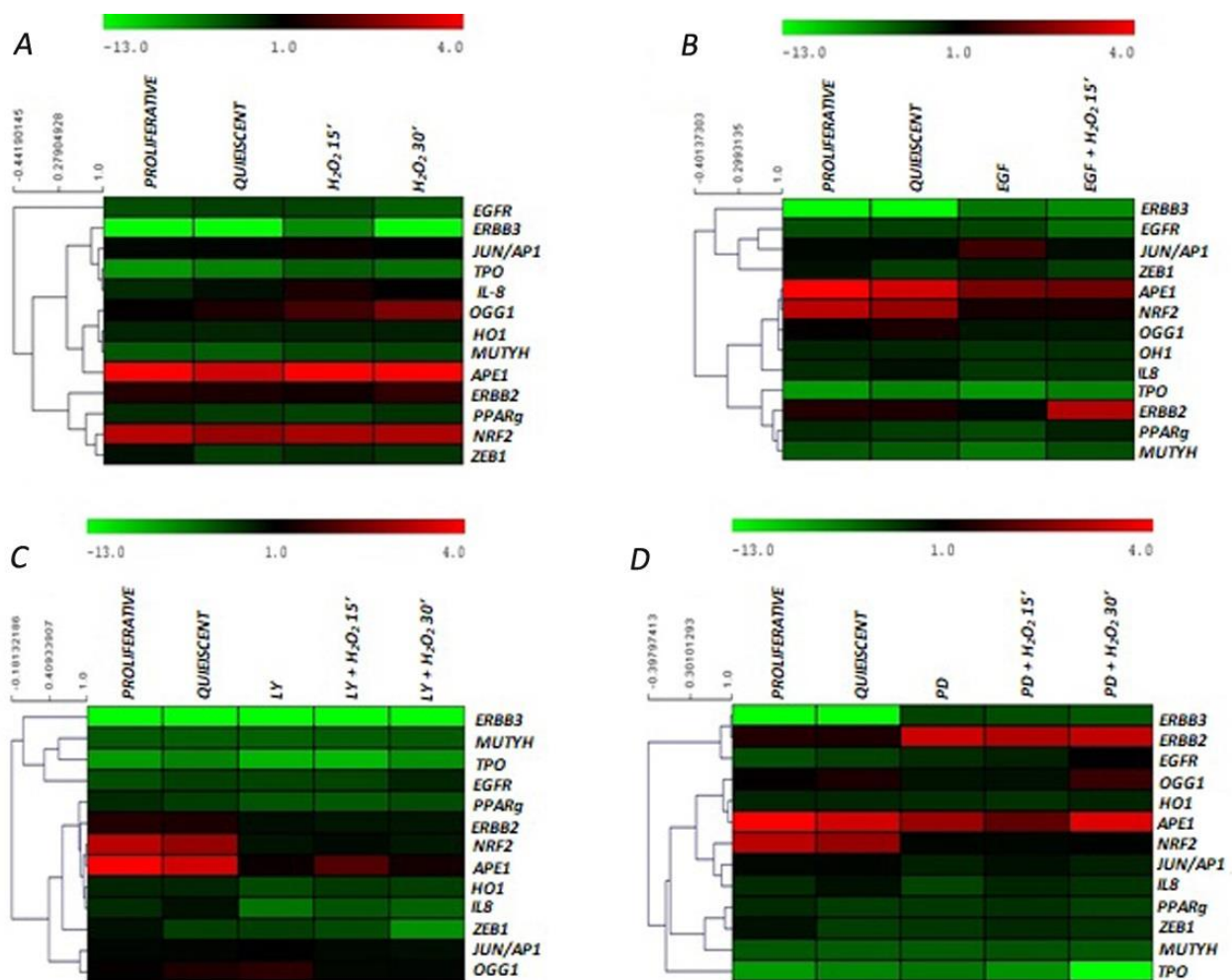


Figure 3. Gene expression cluster analysis by MeV4.9.0 in Nthy-ori 3-1 cells: (A) H₂O₂ treatments; (B) EGF treatments; (C) LY treatments; (D) PD treatments. The average linkage hierarchical clustering with Pearson correlation was used. The colour scale at the top represents the log₂ of every single gene expression value compared to housekeeping value ranging from -13 (green) to 4 (red). The trees presented here are the neighbor-joining trees based on gene expression variation in response of different treatments. LY: LY294002; PD: PD98059

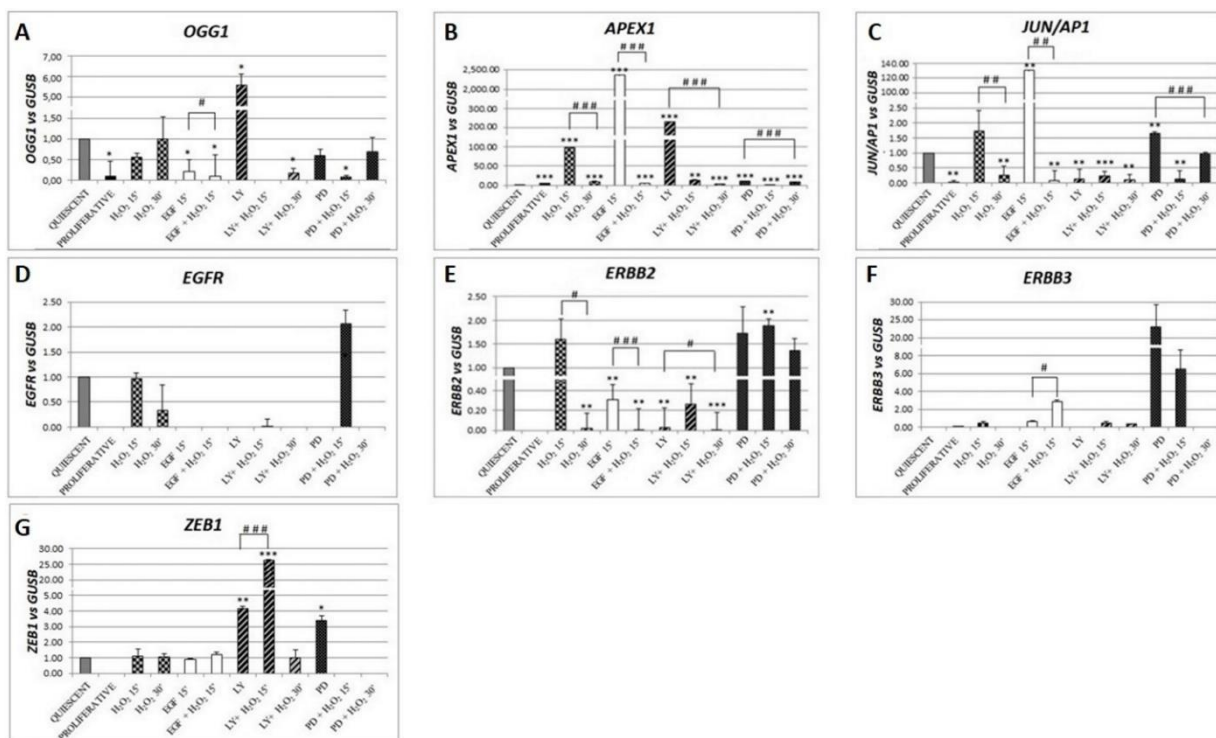


Figure 4. Gene expression modulation under H₂O₂, EGF, LY and PD treatments alone and combined in TPC-1 cells. Gene expression was analysed by Real Time-qPCR. The histogram represented normalized data with GUSB gene, and the results showed the average of three independent experiments. **(A)** *OGG1* (8-Oxoguanine glycosylase); **(B)** *APE1* (apurinic/aprimidinic endodeoxyribonuclease-1); **(C)** *JUN/API* (Jun proto-oncogene, AP-1 transcription factor subunit); **(D)** *EGFR* (epidermal growth factor receptor); **(E)** *ERBB2* (Erb-B2 receptor tyrosine kinase 2); **(F)** *ERBB3* (Erb-B3 receptor tyrosine kinase 3); **(G)** *ZEB-1* (zinc finger E-box binding homeobox 1). LY: LY294002; PD: PD98059

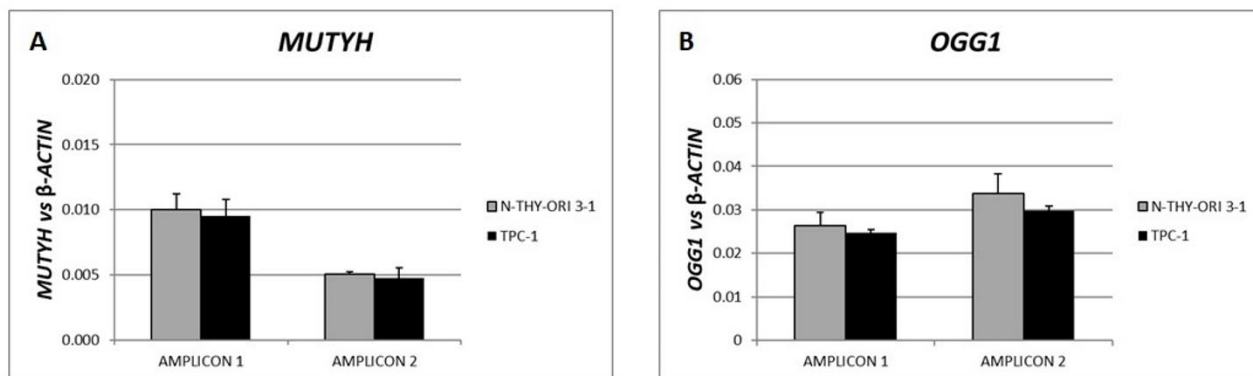


Figure 5. *MUTYH* and *OGG1* gene dosage in Nthy-ori 3-1 and TPC-1 cells. Gene dosage was performed by SYBR Green qRT-PCR. For both genes were selected two different genomic sequences. The samples were amplified in triplicate in three independent experiments. The gDNA amounts of the target genes were normalized by the ratio on median value of the *b-Actin* genomic reference gene from TPC-1 vs Nthy-ori 3-1.

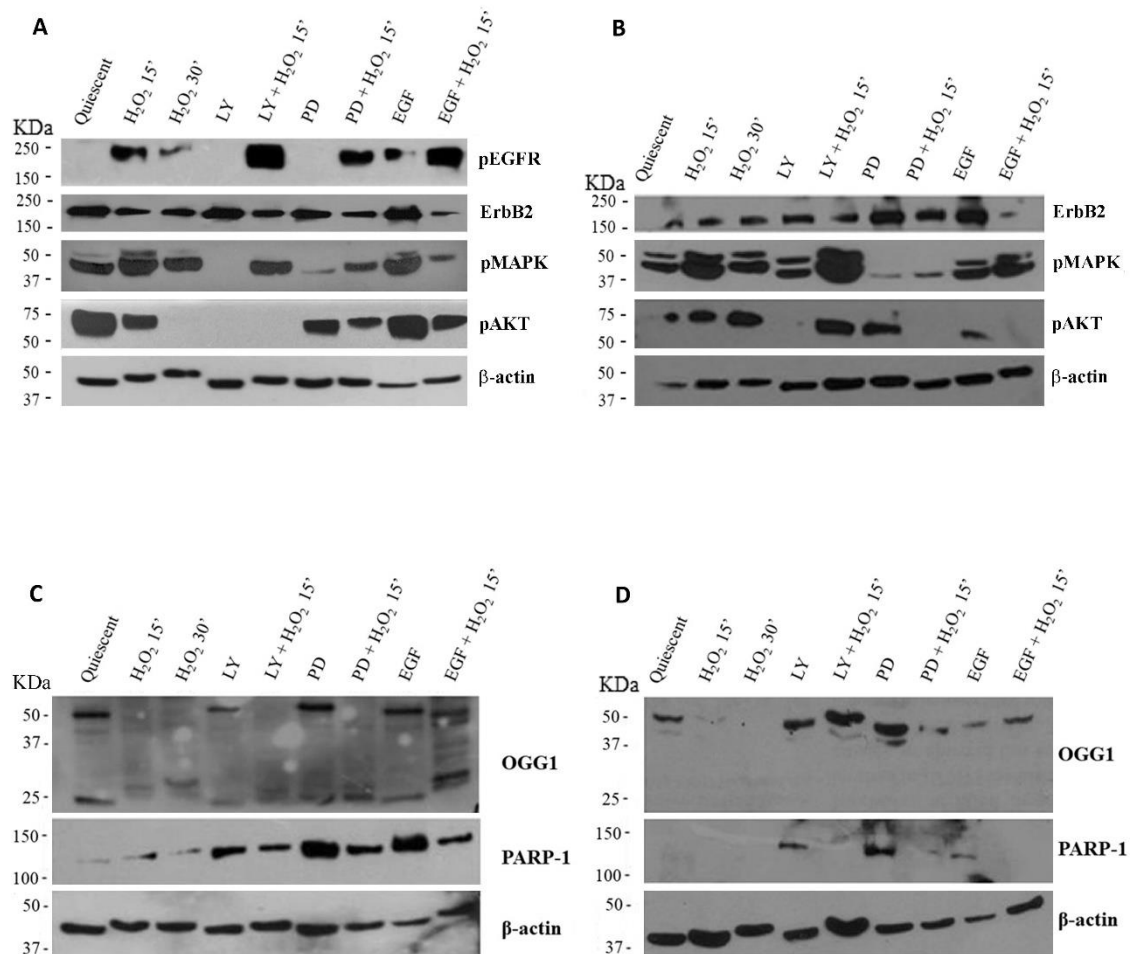


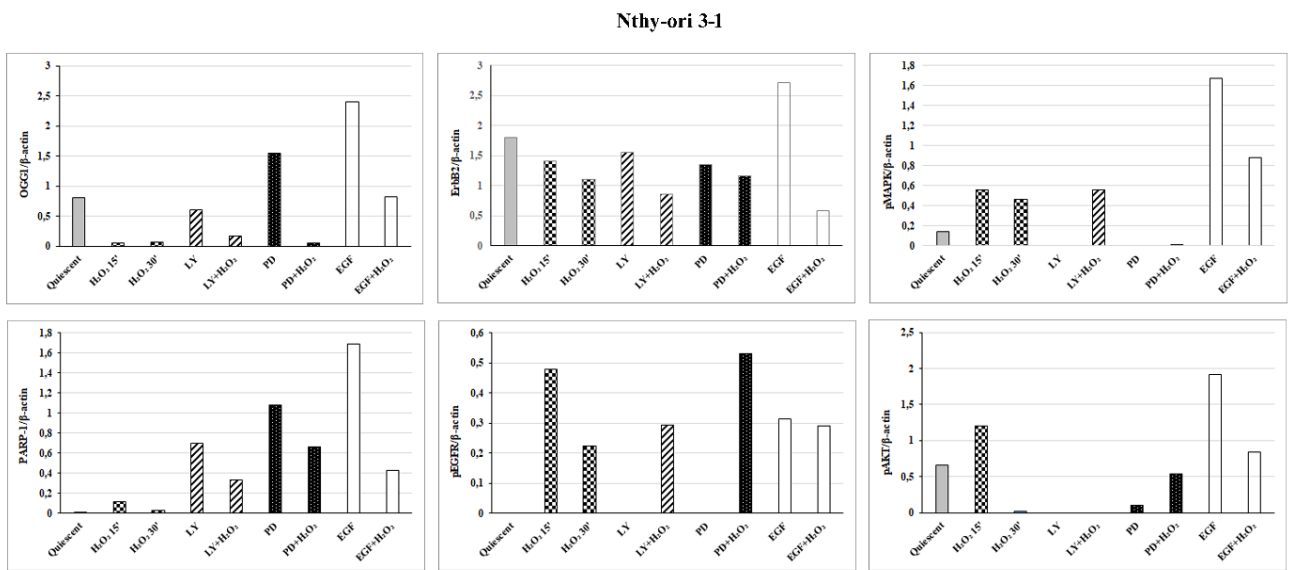
Figure 6: Protein expression of ErbB pathway and OGG1 in Nthy-ori 3-1 and TPC-1 cells.

Nthy-ori 3-1 and TPC-1 cells were starved overnight and treated with, LY294002 (25μM), PD98059 (50μM), EGF (50ng/ml) alone and combined with H₂O₂ (10mM). Western blotting analysis in Nthy-ori 3-1 cells (A-C) and in TPC-1 cells (B-D) determining the protein expression levels of OGG1, PARP-1 (A-B), ErbB2, p-EGFR, p-MAPK, p-AKT (C-D).

Results are representative of three independent experiments.

Q: quiescent cells; LY: LY294002; PD: PD98059.

A



B

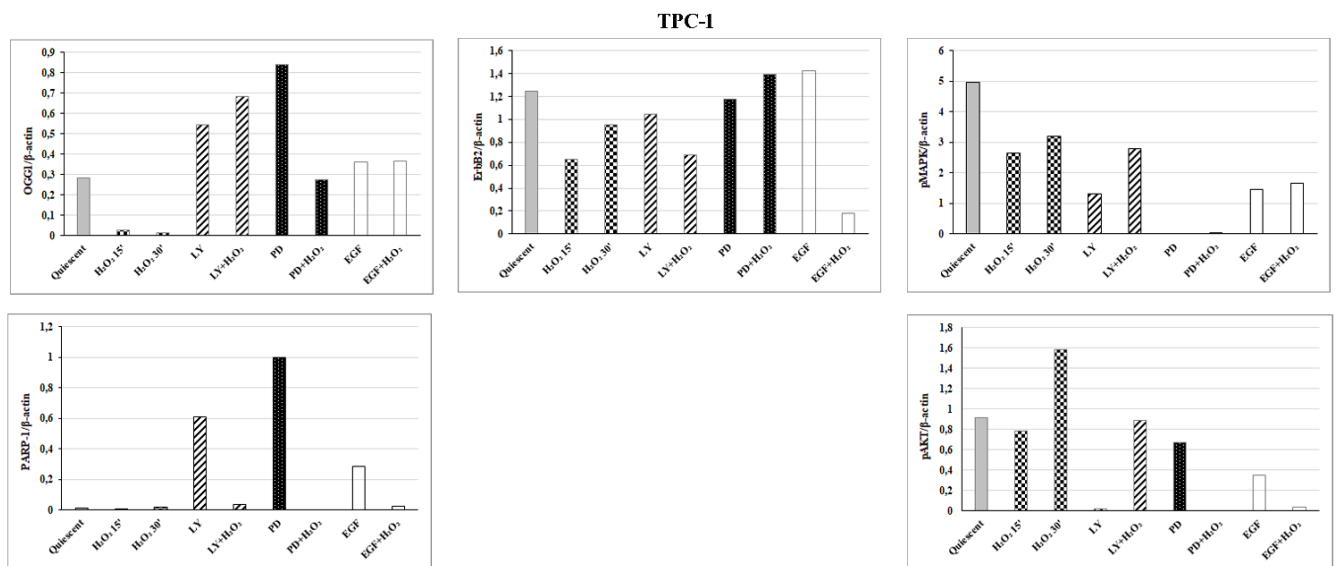


Figure 7: Expression and quantification of selected proteins in Nthy-ori3-1 (panel A) and

TPC-1 (panel B). The average expression levels of panel A and panel B were determined by

densitometric analysis and calculated in relation to the b-Actin level. Quiescent cells were treated

with H₂O₂ and Ly, PD, EGF alone or combined. LY: LY294002; PD: PD98059.

Declaration of Interest

The authors declare that they have no competing interests.

Authors' contributions

CM contributed to study design, gene expression analyses and wrote the Manuscript; MCDM and LS and EDA performed cell cultures and protein analysis; RC, GM and RM critically reviewed the manuscript. GMA designed and coordinated the study and drafted the manuscript.

All authors contributed to data analysis, drafting or revising the article, gave final approval of the version to be published, and agree to be accountable for all aspects of the work.

Funding

This study was supported by the Italian Ministry of Instruction, University and Research (GMA, GM, RC, RM) and by Villa Serena Foundation for Research, Città Sant'Angelo (Pescara), Italy (RC).

Consent for publication

All authors read and approved the final manuscript.

Competing interests

The authors declare that they have no competing interests.

References

- [1] Lim, H.; Devesa, S.S.; Sosa, J.A.; Check, D.; Kitahara, C.M.; Trends in Thyroid Cancer Incidence and Mortality in the United States, 1974-2013. *JAMA*. **2017**, 317, 1338-1348. (doi:10.1001/jama.2017.2719)
- [2] Johnson, N.A.; Tublin, M.E. Postoperative surveillance of differentiated thyroid carcinoma: rationale, techniques, and controversies. *Radiology*. **2008**, 249, 429-44 (doi:10.1148/radiol.2492071313)
- [3] Arora, N.; Scognamiglio, T.; Zhu, B.; Fahey, T.J. Do benign thyroid nodules have malignant potential? An evidence-based review. *World J Surg* **2008**, 32, 1237-1246. (doi:10.1007/s00268-008-9484-1)
- [4] Ameziane El Hassani, R.; Buffet, C.; Leboulleux, S.; Dupuy, C. Oxidative stress in thyroid carcinomas: biological and clinical significance. *Endocr Relat Cancer*. **2019**, 26, R131-R143. (doi: 10.1530/ERC-18-0476)
- [5] Moloney, J.N.; Cotter, T.G. ROS signalling in the biology of cancer. *Semin Cell Dev Biol* **2018**, 80, 50-64. (doi: 10.1016/j.semcdb)
- [6] Ekholm, R. Iodination of thyroglobulin: An intracellular or extracellular process? *Mol. Cell. Endocrinol.* **1981**, 24, 141-163. (doi: 10.1210/er.2015-1090)
- [7] Howie, A.F.; Arthur, J.R.; Nicol, F.; Walker, S.W.; Beech, S.G.; Beckett, G.J. Identification of a 57-kilodalton selenoprotein in human thyrocytes as thioredoxin reductase and evidence that its expression is regulated through the calcium-phosphoinositol signaling pathway. *J. Clin. Endocrinol. Metab.* **1998**, 83, 2052-2058. (doi: 10.1210/jcem.83.6.4875)
- [8] Carvalho, D.P.; Dupuy, C. Thyroid hormone biosynthesis and release. *Mol. Cell. Endocrinol.* **2017**, 458, 6-15. (doi: 10.1016/j.mce.2017.01.038.)

- [9] Sigurdson, A.J.; Hauptmann, M.; Alexander, B.H.; Doody, M.M.; Thomas, C.B.; Struewing, J.P.; Jones, I.M. DNA damage among thyroid cancer and multiple cancer cases, controls, and long-lived individuals. *Mutat. Res.* **2005**, *586*, 173-188. (doi: 10.1016/j.mrgentox.2005.07.001)
- [10] Schieber, M.; Chandel, N.S. TOR signaling couples oxygen sensing to lifespan in *C. Elegans*. *Cell. Rep.* **2014**, *9*, 9-15. (doi: 10.1016/j.celrep.2014.08.075)
- [11] Sies, H. Hydrogen peroxide as a central redox signaling molecule in physiological oxidative stress: Oxidative eustress. *Redox Biol* **2017**, *11*, 613-619. (doi:10.1016/j.redox.2016.12.035)
- [12] Weng, M.S.; Chang, J.H.; Hung, W.Y.; Yang, Y.C.; Chien, M.H. The interplay of reactive oxygen species and the epidermal growth factor receptor in tumor progression and drug resistance. *J. Exp. Clin. Cancer Res.* **2018**, *37*, 61. (doi: 10.1186/s13046-018-0728-0)
- [13] Metere, A.M.; Frezzotti, F.; Graves, C.E.; Vergine, M.; De Luca, A.; Pietraforte, D.; Giacomelli, L.A. Possible role for selenoprotein glutathione peroxidase (GPx1) and thioredoxin reductases (TrxR1) in thyroid cancer: our experience in thyroid surgery. *Cancer Cell Int.* **2018**, *18*, 7. (doi: 10.1186/s12935-018-0504-4)
- [14] Yi, J.W.; Park, J.Y.; Sung, J.Y.; Kwak, S.H.; Yu, J.; Chang, J.H.; Kim, J.H.; Ha, S.Y.; Paik, E.K.; Lee, W.S.; Kim, S.J.; Lee, K.E.; Kim, J.H. Genomic evidence of reactive oxygen species elevation in papillary thyroid carcinoma with Hashimoto thyroiditis. *Endocr. J.* **2015**, *62*, 857-77. (doi:10.1507/endocrj.EJ15-0234)
- [15] Mo, J.Y.; Maki, H.; Sekiguchi, M.; Hydrolytic elimination of a mutagenic nucleotide, 8-oxodGTP by human 18-kilodalton protein: sanitization of nucleotide pool. *Proc. Natl. Acad. Sci. U S A.* **1992**, *89*, 11021-5. (doi: 10.1073/pnas.89.22.11021)
- [16] Oka, S.; Leon, J.; Tsuchimoto, D.; Sakumi, K.; Nakabeppu, Y. MUTYH, an adenine DNA glycosylase, mediates p53 tumor suppression via PARP-dependent cell death. *Oncogenesis* **2015**, *4* e142. (doi: 10.1038/oncsis.2015.4.)
- [17] Banda, D.M.; Nuñez, N.N.; Burnside, M.A.; Bradshaw, K.M.; David, S.S.; Repair of 8-oxoG:A mismatches by the MUTYH glycosylase: Mechanism, metals and medicine. *Free Radic. Biol. Med.* **2017**, *107*, 202-215. (doi: 10.1016/j.freeradbiomed.2017.01.008)
- [18] Paschke, R. Molecular pathogenesis of nodular goiter. *Langenbecks Arch. surg.* **2011**, *396*, 1127-397 (doi: 10.1016/j.beem.2017.04.011)
- [19] Svilar, D.; Goellner, E.M.; Almeida, K.H.; Sobol, R.W. Base excision repair and lesion-dependent subpathways for repair of oxidative DNA damage. *Antioxid. Redox Signal* **2011**, *14*, 2491-2507. (doi: 10.1089/ars.2010.3466)
- [20] Wang, R.; Li, C.; Qiao, P.; Xue, Y.; Zheng, X.; Chen, H.; Zeng, X.; Liu, W.; Boldogh, I.; Ba, X. OGG1-initiated base excision repair exacerbates oxidative stress-induced parthanatos. *Cell Death Dis.* **2018**, *9*, 628. (doi: 10.1038/s41419-018-0680-0)
- [21] Mincione, G.; Di Marcantonio, M.C.; Tarantelli, C.; D'Inzeo, S.; Nicolussi, A.; Nardi, F.; Donini, C.F.; Coppa, A. EGF and TGF- β 1 Effects on Thyroid Function. *J. Thyroid Res.* **2011**, 431718. (doi: 10.4061/2011/431718)
- [22] Ely, A.; Bischoff, L.A.; Weiss, V.L. Wnt signaling in thyroid homeostasis and carcinogenesis. *Genes (Basel)* **2018**, *9*, 204. (doi: 10.3390/genes9040204)

- [23] Chen, D.J.; Nirodi, C.S. The epidermal growth factor receptor: a role in repair of radiation-induced DNA damage. *Clin. Cancer Res.* **2007**, *13*, 6555-6560. (doi:10.1158/1078-0432.CCR-07-1610)
- [24] Bensimon, A.; Aebersold, R.; Shiloh, Y. Beyond ATM: the protein kinase landscape of the DNA damage response. *FEBS Lett.* **2011**, *585*, 1625-1639. (doi: 10.1016/j.febslet.2011.05.013)
- [25] Oberthür, R.; Seemann, H.; Gehrig, J.; Rave-Fränk, M.; Bremmer, F.; Halpape, R.; Conradi, L.C.; Scharf, J.G.; Burfeind, P.; Kaulfuß, S. Simultaneous inhibition of IGF1R and EGFR enhances the efficacy of standard treatment for colorectal cancer by the impairment of DNA repair the induction of cell death. *Cancer. Lett.* **2017**, *407*, 93-105. (doi: 10.1016/j.canlet.2017.08.009)
- [26] Szanto, I.; Pusztaszeri, M.; Mavromati, M. H₂O₂ Metabolism in Normal Thyroid Cells and in Thyroid Tumorigenesis: Focus on NADPH Oxidases. *Antioxidants (Basel)* **2019**, *8*, 126. (doi:10.3390/antiox8050126)
- [27] Saiselet, M.; Floor, S.; Tarabichi, M.; Dom, G.; Hébrant, A.; van Staveren, W.C.; Maenhaut, C. Thyroid cancer cell lines: an overview. *Front. Endocrinol. (Lausanne)* **2012**, *3*, 133. (doi:10.3389/fendo.2012.00133)
- [28] Nicolussi, A.; D'Inzeo, S.; Mincione, G.; Buffone, A.; Di Marcantonio, M.C.; Cotellese, R.; Cichella, A.; Capalbo, C.; Di Gioia, C.; Nardi, F.; Giannini, G.; Coppa, A. PRDX1 and PRDX6 are repressed in papillary thyroid carcinomas via BRAF V600E-dependent and -independent mechanisms. *Int. J. Oncol.* **2014**, *44*, 548-556. (doi:10.3892/ijo.2013.2208)
- [29] Pirkmajer, S.; Chibalin, A.V. Serum starvation: caveat emptor. *Am. J. Physiol. Cell. Physiol.* **2011**, *301*, C272-9. (doi: 10.1152/ajpcell.00091.2011.)
- [30] Aceto, G.M.; Fantini, F.; De Iure, S.; Di Nicola, M.; Palka, G.; Valanzano, R.; Di Gregorio, P.; Stigliano, V.; Genuardi, M.; Battista, P.; Cama, A.; Curia, M.C. Correlation between mutations and mRNA expression of APC and MUTYH genes: new insight into hereditary colorectal polyposis predisposition. *J. Exp. Clin. Cancer Res.* **2015**, *34*, 131. (doi: 10.1186/s13046-015-0244-4)
- [31] Saeed, A.I.; Sharov, V.; White, J.; Li, J.; Liang, W.; Bhagabati, N.; Braisted, J.; Klapa, M.; Currier, T.; Thiagarajan, M.; Sturn, A.; Snuffin, M.; Rezzantsev, A.; Popov, D.; Ryltsov, A.; Kostukovich, E.; Borisovsky, I.; Liu, Z.; Vinsavich, A.; Trush, V.; Quackenbush, J. TM4: a free, open-source system for microarray data management and analysis. *Biotechniques* **2003**, *34*, 374-378. (doi:10.2144/03342mt01)
- [32] Furihata, C. An active alternative splicing isoform of human mitochondrial 8-oxoguanine DNA glycosylase (OGG1). *Genes Environ.* **2015**, *37* 21. (doi: 10.1186/s41021-015-0021-9.)
- [33] Böttcher, Y.; Eszlinger, M.; Tönjes, A.; Paschke, R. The genetics of euthyroid familial goiter. *Trends Endocrinol. Metab.* **2005**, *16*, 314-9. (doi: 10.1016/j.tem.2005.07.003)
- [34] Yarden, Y.; Sliwkowski, M.X. Untangling the ErbB signalling network. *Nat. Rev. Mol. Cell Biol.* **2001**, *2*, 127-37. (doi: 10.1038/35052073)
- [35] Gorrini, C.; Harris, I.S.; Mak, T.W. Modulation of oxidative stress as an anticancer strategy. *Nat. Rev. Drug Discov.* **2013**, *12*, 931-47. (doi: 10.1038/nrd4002)

- [36] Knobel, M.; Medeiros-Neto, G. An outline of inherited disorders of the thyroid hormone generating system. *Thyroid* **2003**, 13, 771-801. (doi: 10.1089/105072503768499671)
- [37] Kim, K.C.; Lee, I.K.; Kang, K.A.; Cha, J.W.; Cho, S.J.; Na, S.Y.; Chae, S.; Kim, H.S.; Kim, S.; Hyun, J.W. 7,8-Dihydroxyflavone suppresses oxidative stress-induced base modification in DNA via induction of the repair enzyme 8-oxoguanine DNA glycosylase-1. *Biomed. Res. Int.* **2013** 863720 (doi: 10.1155/2013/863720)
- [38] Loboda, A.; Damulewicz, M.; Pyza, E.; Jozkowicz, A.; Dulak, J. **2016** Role of Nrf2/HO-1 system in development, oxidative stress response and diseases: an evolutionarily conserved mechanism. *Cell Mol Life Sci* 3221-3247. (doi: 10.1007/s00018-016-2223-0)
- [39] Wang, L.; Jiang, H.; Yin, Z.; Aschner, M.; Cai, J. Methylmercury toxicity and Nrf2-dependent detoxification in astrocytes. *Toxicol. Sci.* **2009**, 107, 135-143. (doi: 10.1093/toxsci/kfn201)
- [40] Natarajan, R.; Gupta, S.; Fisher, B.J.; Ghosh, S.; Fowler, A.A. 3rd. Nitric oxide suppresses IL-8 transcription by inhibiting c-Jun N-terminal kinase-induced AP-1 activation. *Exp. Cell. Res.* **2001**, 266, 203-12. (doi: 10.1006/excr.2001.5218)
- [41] Paszti-Gere, E.; Szeker, K.; Csibrik-Nemeth, E.; Csizinszky, R.; Marosi, A.; Palocz, O.; Farkas, O.; Galfi, P. Metabolites of *Lactobacillus plantarum* 2142 prevent oxidative stress-induced overexpression of proinflammatory cytokines in IPEC-J2 cell line. *Inflammation.* **2012**, 35, 1487-1499. (doi: 10.1007/s10753-012-9462-5)
- [42] Waugh, D.J.; Wilson, C. The interleukin-8 pathway in cancer. *Clin. Cancer Res.* **2008**, 14, 6735-6741. (doi: 10.1158/1078-0432.CCR-07-4843)
- [43] Weetman, A.P.; Bennett, G.L.; Wong, W.L. Thyroid follicular cells produce interleukin-8. *J Clin. Endocrinol. Metab.* **1992**, 75, 328-30. (doi: 10.1210/jcem.75.1.1619027)
- [44] Menendez, J.A. Fine-tuning the lipogenic/lipolytic balance to optimize the metabolic requirements of cancer cell growth: molecular mechanisms and therapeutic perspectives. *Biochim. Biophys. Acta.* **2010**, 1801, 381-391. (doi: 10.1016/j.bbali.2009.09.005)
- [45] Carter, R.J.; Parsons, J.L. Base Excision Repair a Pathway Regulated by Posttranslational Modifications. *Mol. Cell. Biol.* **2016**, **36**, 1426-1437. (doi: 10.1128/MCB.00030-16.)
- [47] Ko, H.L.; Ren, E.C. Functional Aspects of PARP1 in DNA Repair and Transcription. *Biomolecules.* **2012**, 2, 524-48. (doi: 10.3390/biom2040524)
- [46] Noren Hooten, N.; Kompaniez, K.; Barnes, J.; Lohani, A.; Evans, M.K. Poly (ADP-ribose) polymerase 1 (PARP-1) binds to 8-oxoguanine-DNA glycosylase (OGG1). *J. Biol. Chem.* **2011**, 286, 44679-44690. (doi:10.1074/jbc.M111.255869)
- [48] Curia, M.C.; Catalano, T.; Aceto, G.M. MUTYH: Not just polyposis. *World J. Clin. Oncol.* **2020**, 11, 428-449. (doi:10.5306/wjco.v11.i7.428.)
- [49] Frasca, F.; Vella, V.; Nicolosi, M.L.; Messina, R.L.; Gianì, F.; Lotta, S.; Vigneri, P.; Regalbuto, C.; Vigneri, R. Thyroid cancer cell resistance to gefitinib depends on the constitutive oncogenic activation of the ERK pathway. *J Clin Endocrinol Metab.* **2013**, 98, 2502-12. (doi:10.1210/jc.2012-3623)
- [50] Borrello, M.G.; Alberti, L.; Fischer, A.; Degl'innocenti, D.; Ferrario, C.; Gariboldi, M.; Marchesi, F.; Allavena, P.; Greco, A.; Collini, P.; Pilotti, S.; Cassinelli, G.; Bressan, P.; Fugazzola, L.; Mantovani, A.; Pierotti, M.A. Induction of a proinflammatory program in normal human thyrocytes by the RET/PTC1 oncogene. *Proc. Natl. Acad. Sci. U S A* **2005**, 102, 14825-30. (doi:10.1073/pnas.0503039102)

- [51] Mabley, J.G.; Pacher, P.; Deb, A.; Wallace, R.; Elder, R.H.; Szabó, C.; Potential role for 8-oxoguanine DNA glycosylase in regulating inflammation. *FASEB J.* **2005**, *19*, 290-2. (doi: 10.1096/fj.04-2278fje).
- [52] Li, G.; Yuan, K.; Yan, C.; Fox, J. 3rd.; Gaid, M.; Breitwieser, W.; Bansal, A.K.; Zeng, H.; Gao, H.; Wu, M., 8-Oxoguanine-DNA glycosylase 1 deficiency modifies allergic airway inflammation by regulating STAT6 and IL-4 in cells and in mice. *Free Radic Biol Med.* **2012**, *52*, 392-401. (doi: 10.1016/j.freeradbiomed.2011.10.490)
- [53] Bacsi, A.; Aguilera-Aguirre, L.; Szczesny, B.; Radak, Z.; Hazra, T.K.; Sur, S.; Ba, X.; Boldogh, I., Down-regulation of 8-oxoguanine DNA glycosylase 1 expression in the airway epithelium ameliorates allergic lung inflammation. *DNA Repair (Amst).* **2013**, *12*, 18-26. (doi: 10.1016/j.dnarep.2012.10.002)
- [54] Ba, X.; Aguilera-Aguirre, L.; Rashid, Q.T.; Bacsi, A.; Radak Z.; Sur, S; Hosoki, K.; Hegde, M.L.; Boldogh, I. The role of 8-oxoguanine DNA glycosylase-1 in inflammation. *Int. J. Mol. Sci.* **2014**, *15*, 16975-97. (doi: 10.3390/ijms150916975)
- [55] Kim, D.W.; Hwang, J.H.; Suh, J.M.; Kim, H.; Song, J.H.; Hwang, E.S.; Hwang, I.Y.; Park, K.C.; Chung, H.K.; Kim, J.M.; Park, J.; Hemmings, B.A.; Shong, M. RET/PTC (rearranged in transformation/papillary thyroid carcinomas) tyrosine kinase phosphorylates and activates phosphoinositide-dependent kinase1 (PDK1): an alternative phosphatidylinositol 3-kinase-independent pathway to activate PDK1. *Mol. Endocrinol.* **2003**, *17*, 1382-94. (doi:10.1210/me.2002-0402)
- [56] Oka, S.; Nakabeppu, Y. DNA glycosylase encoded by MUTYH functions as a molecular switch for programmed cell death under oxidative stress to suppress tumorigenesis. *Cancer Sci.* **2011**, *102*, 677-82. (doi: 10.1111/j.1349-7006.2011.01869.x.)
- [57] Uddin, M.A.; Akhter, M.S.; Siejka, A.; Catravas, J.D.; Barabutis, N. P53 supports endothelial barrier function via APE1/Ref1 suppression. *Immunobiology.* **2019**, *224*, 532-538. (doi:10.1016/j.imbio.2019.04.008)